

# Characterization And Activity Evaluation Of Acidic Zeolites: Valorization Of Glycerol To Solketal, A Fuel Additive

Yadaiah Salwadi<sup>1</sup>, Venkatesham Kothabai<sup>1</sup>, Vijayalaxmi Burri<sup>1</sup>,  
Balakrishna Matkala<sup>1,2</sup> Sasikumar Boggala<sup>3</sup> And Hari Padmasri Aytam<sup>1\*</sup>

<sup>1</sup>Department Of Chemistry, Osmania University, Hyderabad-500 007, Telangana, India.

<sup>2</sup>Department Of Chemistry, SR & BGNR Govt. Arts & Science College (A), Khammam, Telangana, India

<sup>3</sup>Catalysis & Fine Chemicals Department, CSIR-Indian Institute Of Chemical Technology, Hyderabad-500 007, Telangana, India

---

## Abstract:

Solketal is a value added product obtained by acetalization of glycerol, a by-product obtained in the bio-diesel production. Simple zeolites viz., Beta, Y, ZSM5 and Ferrierite were acidified to achieve good yields of solketal under mild reaction conditions in this study. All the acidic zeolites were characterized by XRD, SEM-EDAX, BET-SA, FT-IR, Raman, XPS and Py-IR to understand their physical, morphological and chemical nature. Among the four zeolites studied in comparison at optimized reaction conditions, HZSM5 showed better activity. The order of activity of the catalysts was in line with their acidity. All the zeolites studied showed a stable activity even after 4 cycles of reaction run.

**Keywords:** Glycerol, Solketal, Zeolites, Acetalization, Acidity

---

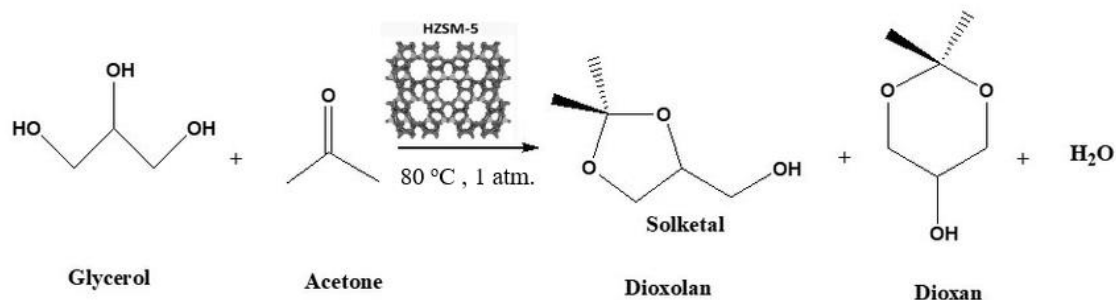
Date of Submission: 28-11-2023

Date of Acceptance: 08-12-2023

---

## I. INTRODUCTION

Paris Treaty that came into enforcement in 2016 adopted by 196 countries at the UN Climate Change Conference (COP21) sparked up low carbon solutions with a goal to reduce 70% global emissions by 2030. One of the major sectors that contribute to the emissions is fuels which are traditionally are obtained from non-renewable resources and high carbon containing molecules. Thus, it is imperative to shift the production methods of fuels and chemicals obtained from the non-renewable feed stocks to more reliable and renewable feed stocks such as biomass. Bio-diesel is renewable fuel that is enviro-friendly in reducing the emission of harmful gases. However, the success of bio-diesel production globally is based on the effective utilization of its by-product, glycerol which is generated at an extent of 10% of the bio-diesel produced [1]. Transformation of glycerol to value added products can turn the bio-diesel process economical viable. Solketal is a value added products with immense applications as a solvent, plasticizer, surfactant, disinfectant and flavoring agent and green fuel additive to bio-diesel [2, 3]. Solketal is synthesized by the acetalization of glycerol by means of both homogeneous as well as heterogeneous catalysis [4-7]. However easy recoverable and more enviro-friendly heterogeneous catalysts are preferred over their homogeneous counterparts for the efficient synthesis of solketal. Several metal oxides, zeolite based, hydrotalcite and other silica materials were used in this respect [8-11]. Our recent reports on modified MCM41 based catalysts showed higher rates of formation of solketal at ambient conditions [12, 13]. Acetalization of glycerol for the selective formation requires acid sites both Lewis as well Bronsted. Heterogeneous catalysts have the added advantage of devising tailor made catalysts with required type and amount of acid sites using variable supports and modifying the basic catalyst to meet the conditions for selective synthesis of products. The present work is an effort placed in the utilization of commercially available zeolites and acidifying them to match with characteristics necessary for the synthesis of solketal in good amounts under mild reaction conditions. Four different acidic zeolites namely HY, HZSM-5, H $\beta$  and HFER were obtained by acidifying the commercial Y, ZSM-5 Beta and FER zeolites. These zeolites were then employed in transformation of glycerol to solketal by acetalization reaction. The reaction conditions were optimized by studying the effect of temperature, reactants' mole ratio effect, variation in catalyst amount and time on scale on the catalytic activity of the acidic zeolites.



**Scheme 1: Glycerol acetalization to solketal over zeolite catalyst**

## II. EXPERIMENTAL METHODS

### Chemicals Used

Glycerol and acetone were of Sigma Aldrich and Spectrochem make of AR grade and used as such in the reaction with no further treatment.

### Preparation of Catalysts

Commercial ammonical form of zeolites Y, ZSM-5, FER and Beta zeolites were purchased from Alfa Aesar. Thus obtained ammonical zeolites were calcined at 500 °C for 5 h to obtain their respective acidic zeolites.

### Characterization Techniques

A Rigaku miniplex powder X-ray diffractometer was used for Powder X-ray diffraction (XRD) analysis with Cu K $\alpha$  (1.5406 Å) radiation source operated at 40kV and 15mA. Surface properties were measured using N<sub>2</sub> adsorption, at -196 °C (Micromeritic ASAP 2010 surface area analyzer) and Scanning Electron Microscopy (FE-SEM) with Energy Dispersive X-ray (EDX) analyzer for elemental distribution was used to study the surface morphology of the catalysts. FT-IR spectra of synthesized catalysts were recorded in the range of 400-4000 cm<sup>-1</sup> on Thermo Nicolet iS50 with inbuilt ATR. Raman Spectra were recorded on a recorded using a 633 nm line from a He-Ne laser and the scattered light was analyzed using HORIBA JOBIN YVON HR800, Japan. The NH<sub>3</sub>-TPD analysis was performed to measure the acidity of the catalysts on an Auto Chem 2910 (Micromeritics).

### Activity evaluation of catalysts

Acetalization of glycerol to solketal was conducted in a batch type glass reactor closed with a septum placed over a magnetic stirrer. The reaction was studied to evaluate the catalytic activity of zeolites taken in variable amounts at different temperatures and mole ratios of reactants in the reactor. At regular intervals of time the reaction mixture was collected and analysed by a GC (Agilent 1020A) equipped with a FID. The products were confirmed by GC-MS. The reaction mixture was centrifuged to separate the catalyst, washed with deionized water and dried in oven at 100 °C overnight in order to test the reusability of the catalysts. The conversion of glycerol ( $X$ ) and selectivity to solketal ( $S$ ) were obtained using the following equations:

$$\text{Conversion of Glycerol } (X_{\text{Gly}}\%): \quad \%X_{\text{Gly}} = \frac{C_{\text{Gly}_0} - C_{\text{Gly}}}{C_{\text{Gly}_0}} \times 100$$

where  $C_{\text{Gly}_0}$  is the molar concentration (mol/L) of glycerol before the reaction and  $C_{\text{Gly}}$  is the molar concentration (mol/L) of glycerol after the reaction

$$\text{Selectivity to Solketal } (S_{\text{Skt}}\%): \quad \%S_{\text{Skt}} = \frac{C_{\text{Skt}}}{C_{\text{Gly}_0} - C_{\text{Gly}}}$$

where  $C_{\text{Skt}}$  is the molar concentration (mol/L) of solketal after the reaction.

## III. RESULTS AND DISCUSSION

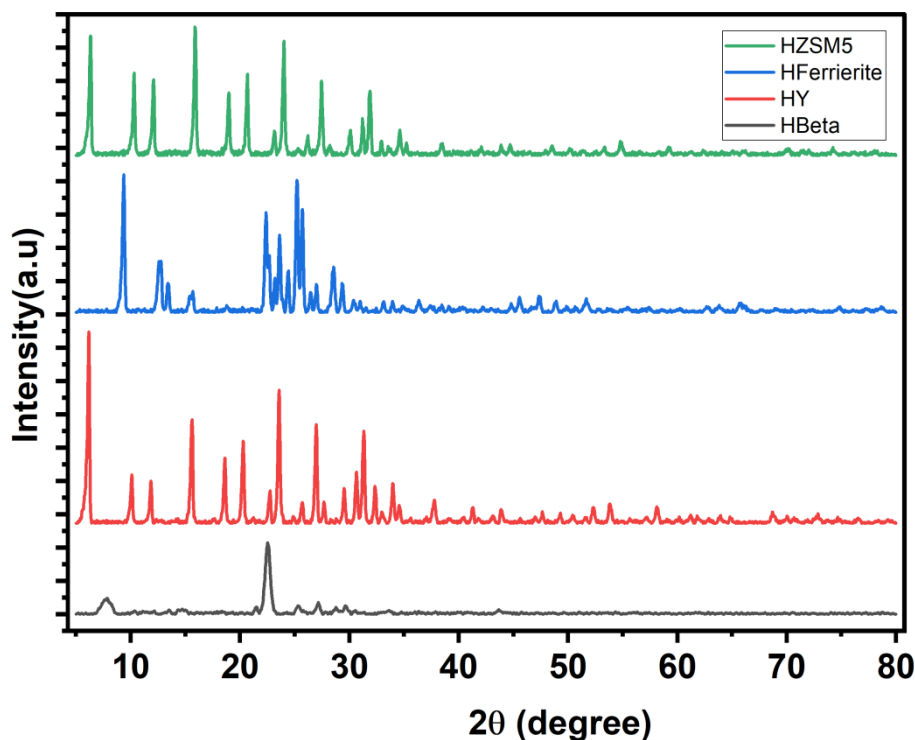
### XRD analysis

Fig.1 indicates the X-ray diffractograms of the four acidic zeolites used in this study. The crystal structure, crystallite size and presence of any defects in the structure of zeolites can be deduced from the XRD analysis. The patterns of HZSM5 show the microcrystalline nature of the sample with matching with the pattern of JCPDS no. 00-037-0359 [14]. Those of H $\beta$  are found to coincide with the  $2\theta$  values = 7.62°, 21.13° and 22.30° reported by W. Zhang et al. [15]. HY X-ray diffractograms are according to the Faujasite structure, JCPDS no. 43-0168 [16]. I. FER is a 10-membered ring zeolite with medium size pores and the report of Capel Berdiell et

al., [17] on XRD of HFER is a good match to the pattern of HFER reported here in fig.1. The Scherrer equation is used to determine the crystallite size of all these zeolites and presented in table 1.

**Table 1: Physico-Chemical Characteristics of Zeolite catalysts**

Zeolite	BET-SA (m <sup>2</sup> g <sup>-1</sup> )		Crystallite Size, nm (from XRD) in H-Form	Total Acidity, m mol(g <sub>cat</sub> ) <sup>-1</sup> in H-Form
	NH <sub>4</sub> -Form	H-Form		
ZSM5	400	370	35.5	0.92
Y	730	705	34.3	0.43
β	600	570	15.8	1.01
FER	400	375	32.8	0.78



**Figure 1: XRD patterns of HZSM5, HFER, Hβ, HY zeolites**

**BET-Surface area**

The surface areas of the catalysts have been measured using BET method by N<sub>2</sub> adsorption at -196 °C. The surface areas as indicated in table 1 shows a slight decrease after calcination from their ammonical form to acidic H-form due to loss in NH<sub>3</sub> as well as water/hydroxyl groups resulting in the decrease in the available surface of the catalysts. The isotherms (not shown) indicated type I kind as expected of the microporous nature of the zeolite materials except for Hβ a variation in isotherm shape as it is known to possess mesopores as well along with micropores. The surface areas of HY and Hβ are higher owing to their larger pores and structure in comparison to the MFI structure of ZSM 5 and Ferrierite zeolites.

**SEM-EDAX Results**

The micrographs from SEM results indicate presence of more dispersed fine particles in case of Beta and Y zeolites owing to their higher specific surface area as compared to other two zeolites. HSM5 and HFER samples also showed uniformly dispersed particles but with slight agglomerization resulting in bigger particles in comparison to H-Beta and HY catalysts. The morphology of the particles is not very clear but certain reports on the SEM analysis of these zeolites show Beta zeolites to be more dispersed assemblies of small homogenous particles whereas the HSZM5 and HY formed by well-formed cubic particles while HFER exhibited plate-like particles formed by inter growth agglomerization [18].

SEM-EDAX Results

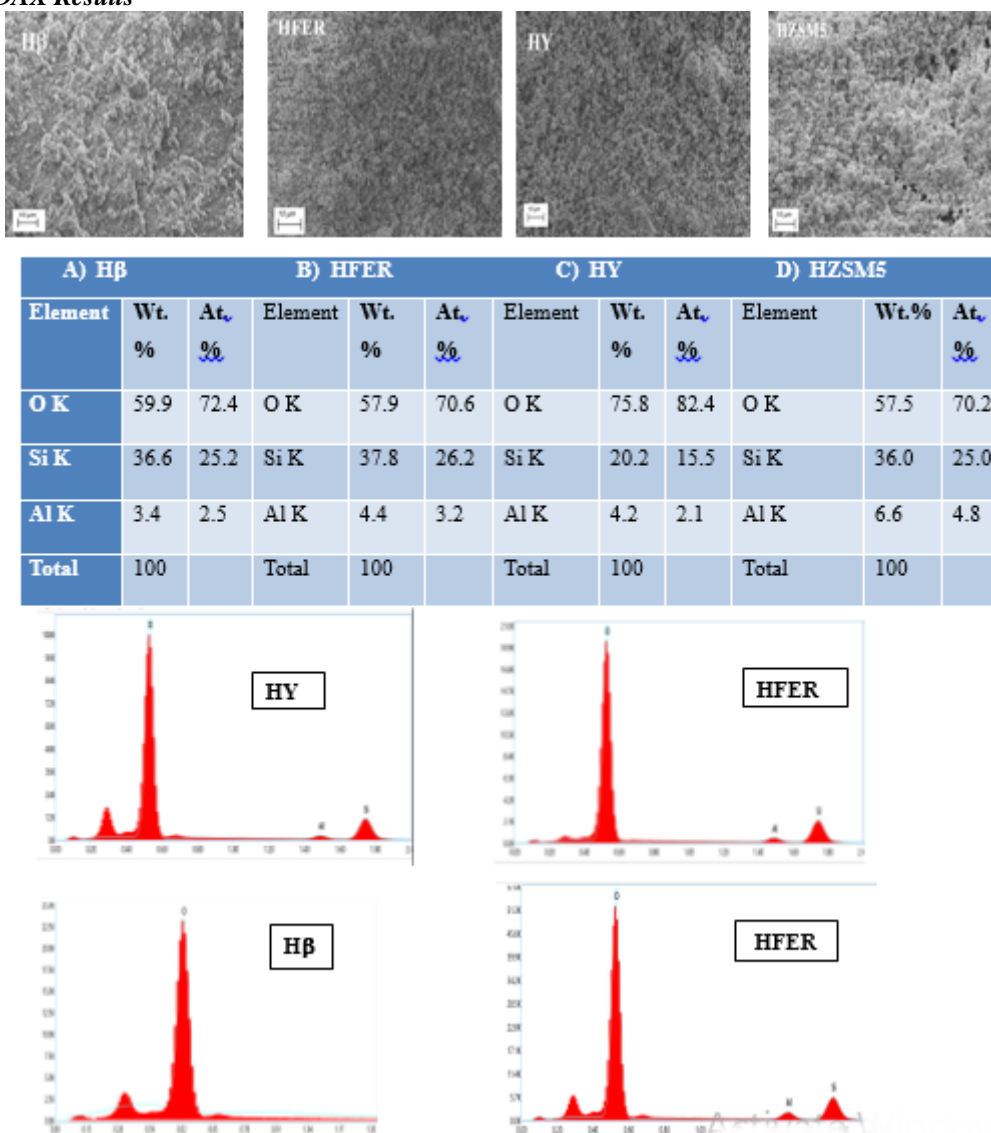


Figure 2: SEM, EDAX Images and Elemental Composition of Acidic Zeolite Catalysts

FT-IR Spectral Data

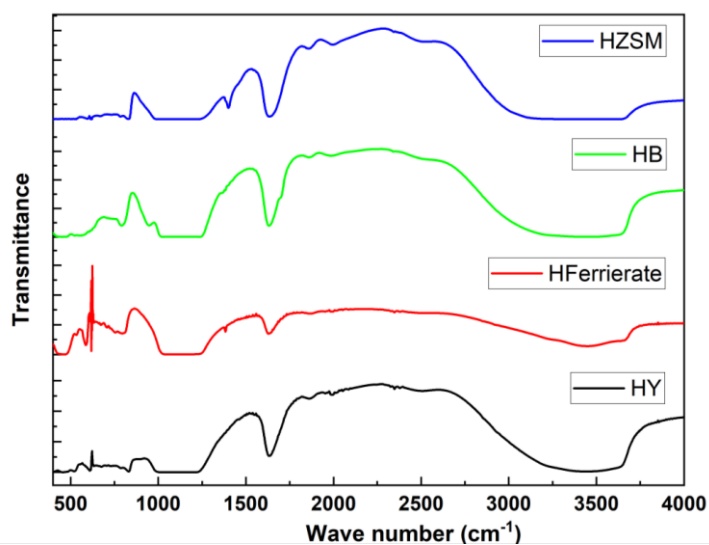
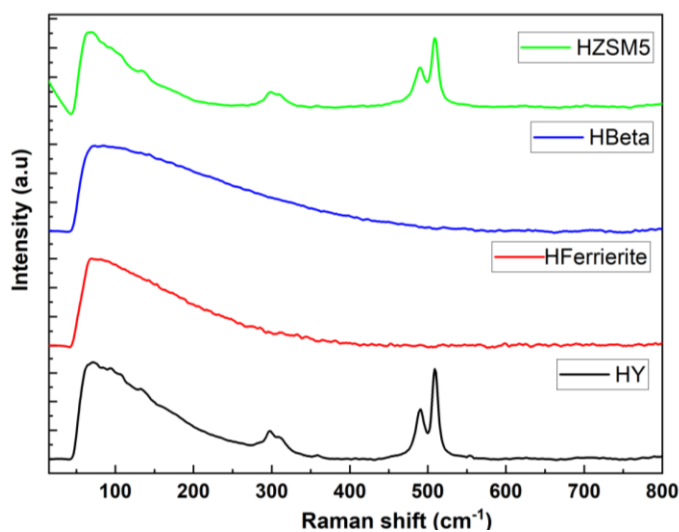


Figure 3: FT-IR spectra of acidic zeolites

The FT-IR spectra of the zeolites show an extensive band centered around 3500-3600  $\text{cm}^{-1}$  attributed to the hydroxyl groups associated with the basic silica framework of the zeolites as depicted in the figure 3. The fundamental -OH stretching modes reported commonly with zeolites in this region i.e., 3610-3750  $\text{cm}^{-1}$  are due to two main distinguishable features of zeolites. The band corresponding to isolated silanol groups on the external surfaces of zeolites at 3750 - 3745  $\text{cm}^{-1}$ , whereas the band at 3610  $\text{cm}^{-1}$  is assigned to the stretching mode of (-Al(OH)Si-) bridging hydroxyl groups [19]. However, these two features are not very clearly distinguished in the FT-IR patterns obtained, though a small bend at 3600  $\text{cm}^{-1}$  is observed. Another distinct peak around 1630  $\text{cm}^{-1}$  is attributed to the bending mode of vibrations of the hydroxyl groups of the zeolites [20].

### **Raman Spectral Analysis**

The figure 4 above depicts the Raman spectra of the acidic forms of the four zeolites used for the acetalization of glycerol. The spectra of HZSM5 and HY zeolites showed characteristic peaks in between 300-500  $\text{cm}^{-1}$  with a broad low frequency band centered  $\sim 80 \text{ cm}^{-1}$  attributed to cation-oxygen vibrational modes [19]. This band appeared in common in all the zeolites with a few  $\text{cm}^{-1}$  variations in the Raman shift in their spectra probably due to the disparity in silica content in these zeolites. The spectra of these two zeolites are nearly similar with slight variation in the intensities of the bands. The two main peaks centered around 495 and 505  $\text{cm}^{-1}$  were due to mixed stretching and bending modes of vibrations of Si-O-Si bonds [20]. The -Si-O- bonds in the zeolites with 4-membered rings were reported to exhibit strong Raman band in the region of 450-550  $\text{cm}^{-1}$ . And as the no. of rings in the zeolites increased the band shifted to lower frequencies with zeolites formed by 6-membered rings showing the bands around 300-350  $\text{cm}^{-1}$  while those with eight membered rings gave bands at even lower wave numbers of 200-250  $\text{cm}^{-1}$ . This very well correlate to the Raman spectra of the present study with HZSM5 formed by 10-membered rings and HY, H $\beta$  constituting 12-membered rings showed maximum shift to lower wave number as seen in figure 4.



**Figure 4: Raman spectra of acidic zeolites**

### **Acidity Measurements**

Two desorption peaks could be mainly seen in the TPD patterns of  $\text{NH}_3$  (figure not shown), one around 400-500 K which is more intense and another  $\sim 600-700 \text{ K}$  which is more broad. Based on the temperature of desorption generally the peaks are attributed to weak acidic sites at lower temperatures and to strong acid sites at higher temperature. Thus, the lower temperature peak observed in TPD patterns may be designated as weak while that at higher temperature of 600-700 K as to strong acidity over the zeolite catalysts. TPD technique cannot distinguish the type of acid sites. However, the reports on the acidity of the catalysts show from the py-IR studies that zeolites possess both Bronsted and Lewis acid sites [22] that could be seen binding to pyridine in both protonated form (band at 1456  $\text{cm}^{-1}$ ) over Bronsted acid sites as well coordinated to Lewis acid sites through the lone pair of electrons on the nitrogen of pyridine (band at 1452  $\text{cm}^{-1}$ ).

### **Activity Evaluation**

The catalytic performance of the four acidic zeolites viz., HZSM5, HFER, HY and H $\beta$  was evaluated for the acetalization of glycerol in the selective synthesis of solketal, a fuel additive. The temperature effect studied over these catalysts at ambient conditions of pressure with a mole ratio of glycerol:acetone = 1:10 and

using 100 mg of catalyst as can be seen from figure 5 indicates 80 °C as optimum temperature to attain maximum conversion of glycerol and hence higher yields to solketal. And among the different zeolites studied H $\beta$ /HZSM5 were found to be more efficient in terms of higher rate of formation of solketal indicated in figure 6, attributed to its superior acidity against the rest three of the zeolites. The other reaction conditions viz., mole ratios of reactants, amount of catalyst used and time on stream were also studied.

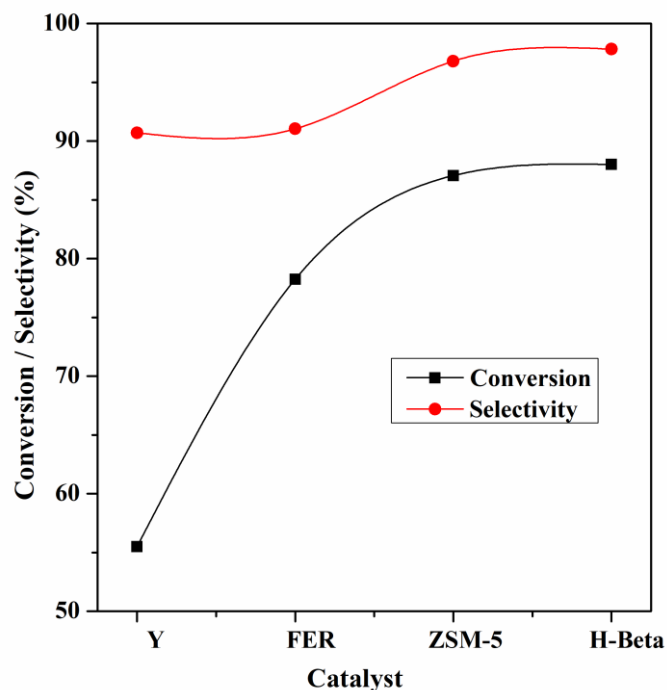


Figure 5: Acetalization of glycerol over acidic zeolites at optimized reaction conditions

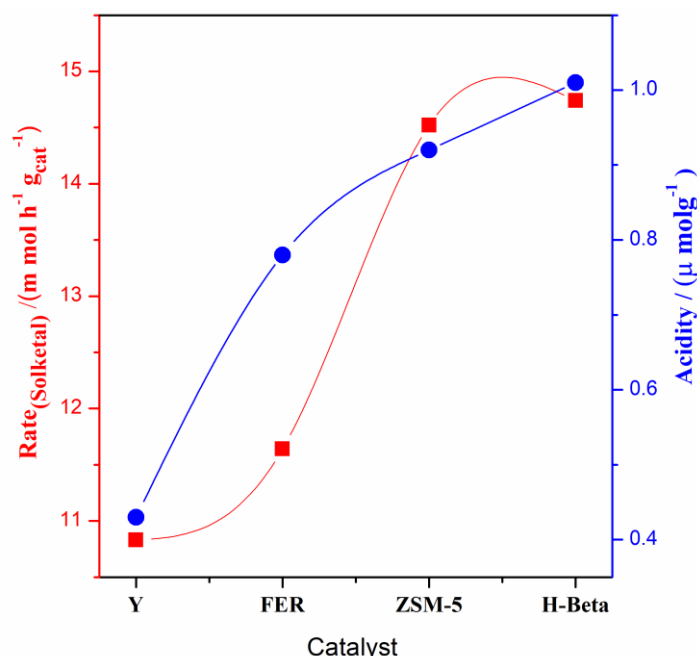


Figure 6: Rate of formation of solketal over acidic zeolite catalysts as a function of their total acidity at optimized reaction conditions

The figures 7, 8 and 9 clearly show these variations studied over the catalyst and it can be inferred that the reaction rate is enhanced with rise in temperature from room temperature to 80 °C that can be seen in the enhanced conversion levels and also selectivity to desired products. The six membered acetal compound was obtained as the by-product in small amounts as evidenced from the GC-MS analysis of the product mixture. A

mole ratio of glycerol:acetone = 1:10 with 100 mg of catalyst and steady state activity at 180 min. are optimum to obtain higher yields of the desired product, solketal. The catalyst amount was varied from 50 mg to 125 mg. As the catalyst amount is increased an obvious increase in the yields of the desired product could be evidenced with the availability of increased no. of active sites of the catalyst. However after 100 mg there was not much change seen that indicates 100 mg catalyst amount is optimum and sufficient enough to achieve maximum yields of solketal over the best catalyst studied i.e., HZSM 5. The studies on glycerol acetalization using acetone report higher molar ratios of these two reactants to be required due to the lower solubility of glycerol in acetone where acetone plays the roles of both reactant as well as the solvent in this reaction [23].

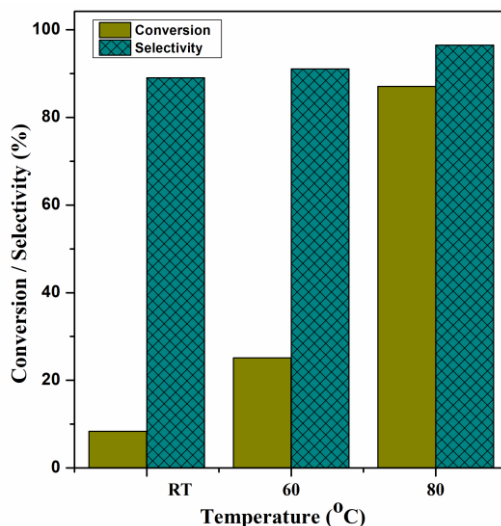


Figure 7: Effect of temperature on glycerol acetalization over HZSM-5 (at glycerol:acetone = 1:10; 1 atm.; 100 mg cat.)

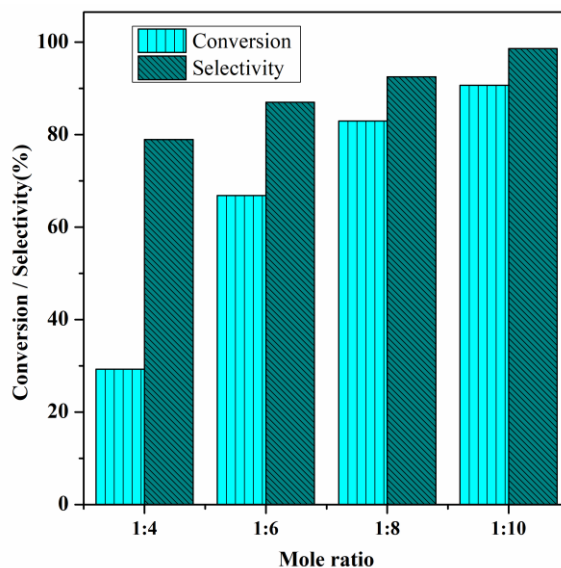


Figure 8: Effect of mole ratio of glycerol:acetone in the synthesis of solketal from glycerol over HZSM-5 (at 80 °C; 1 atm.; 100 mg cat.)

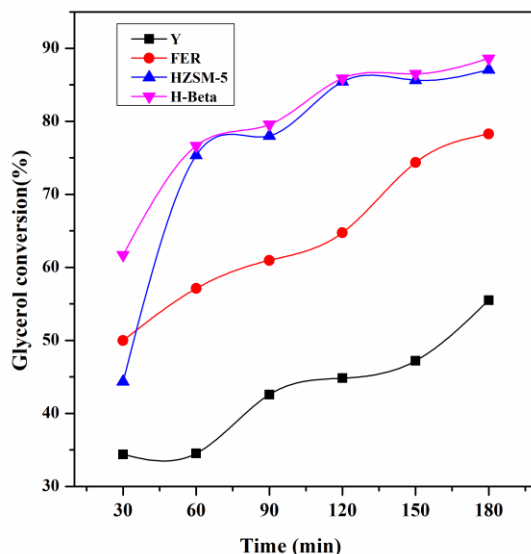


Figure 9: Time on stream studies on glycerol acetalization over HZSM-5 catalyst

The reusability studies carried out at optimum reaction conditions over the acidic zeolites for the glycerol acetalization depicted in figure 10 illustrates good stability of these catalysts even after 4 runs of the reaction. However, HZSM-5 showed better stability among the two catalysts that showed higher activity towards solketal formation i.e., among HZSM-5 and H $\beta$ . Though H $\beta$  possessed higher acidity among all the four zeolites, the catalytic performance of HZSM-5 was nearly the same that of H $\beta$  and it was found to be more stable in terms of uniform activity that was nearly the same even after 5 runs of reaction. However, H $\beta$  showed slight loss in activity after 2-3 though retained much considerable activity even after 5<sup>th</sup> reaction run. This probably may be attributed to the greater strength of acid sites on this zeolite that might be leading to deactivation or loss in activity of the catalyst with time. The catalysts were centrifuged, filtered, washed with acetone/deionized water and dried in an oven at 100 °C before every run to avoid any deactivation possible with the traces of adsorbed reactants/products on the surface of the catalysts. The XRD data (not shown) obtained after the reaction which shows no change in the patterns is indicative of intact structures that further establishes the stability of the zeolites used in the study.

Glycerol acetalization reaction requires both Lewis (L) and Bronsted (B) acid sites. The reaction mechanism reported [13, 24] established the higher selectivity attributed to greater Lewis acid sites on the surface of catalysts though the initial activation of carbonyl group of acetone can take place on either of the L/B sites and further steps of dehydration and cyclization results in a more kinetically favoured 5-membered ring product, solketal. The present findings on acidic zeolites also confirm and re-establish the same. The other by-product formed in smaller amounts is the 6-membered ring, acetal product.

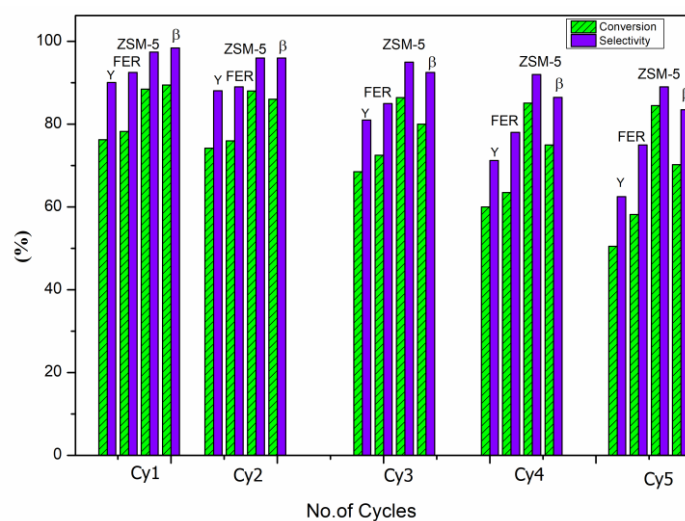


Figure 10: Reusability studies in the acetalization of glycerol over acidic zeolites under optimized reaction conditions.



#### IV. CONCLUSIONS

Simple acidic zeolites were demonstrated to show good activity in the valorization of glycerol to solketal by acetalization under mild reaction conditions. The characterization of the acidic zeolites revealed microcrystalline and microporous nature with good surface area as revealed from the XRD and BET-surface area measurements. The SEM micrographs show uniform particle size with H $\beta$  showing smaller particles owing its higher surface area. Raman analysis clearly indicated the difference in the vibrational modes corresponding to the various Si-O-Si stretching and bending vibrations that vary with the size, no. of rings and arrangement of the tetrahedral units that make up the ring structure of the four different zeolites. The acidity measurements correlate to the activity of the catalysts for the acetalization reaction studied. H $\beta$ /HZSM5 that exhibited higher acidity, higher porosity and stability is found to be more efficient in yielding the desired product, solketal at higher rates of formation over the rest of the zeolites. The acetalization activity of these zeolites was found to be in the order of their acidity. All the zeolite catalysts exhibited stable activity and recyclability for 4 cycles of reaction run.

#### ACKNOWLEDGEMENTS

The authors thank Dr. A. Venugopal, Chief Scientist, C & FC Department, CSIR-IICT, Hyderabad, India for some of the characterization of the catalysts.

#### REFERENCES

- [1]. D.T Johnson, K.A Taconi, Environ. Prog. 26 (2007) 338–348.
- [2]. C.-H. (Clayton) Zhou, J.N. Beltramini, Y.-X. Fan, G.Q. (Max) Lu, Chem. Soc. Rev. 37 (2008) 527–549.
- [3]. R. Sarkari, Ch. Anjaneyulu, V. Krishna, R. Kishore, M. Sudhakar, A. Venugopal, Catal. Commun. 12 (2011) 1067–1070.
- [4]. L. Chen, B. Nohair, D. Zhao, S. Kaliaguine, Appl. Catal. A: Gen. 549 (2018) 207-215.
- [5]. M.N. Timofeeva, V.N. Panchenko, N.A. Khan, Z. Hasan, I.P. Prosvirin, S.V. Tsybulya, S.H. Jung, Appl. Catal. A: Gen. 529 (2017) 167-174.
- [6]. Z. Li, Z. Miao, X. Wang, J. Zhao, J. Zhou, Si W, S. Zhuo, Fuel 233 (2018) 377-387.
- [7]. M.S. Khayoon, B.H. Hameed, Appl. Catal. A: Gen. 464 (2013) 191-199.
- [8]. A. Da Silva, V.L.C. Goncalves, C.J.A. Mota, Green Chem. 11 (2009) 38–41.
- [9]. B. Mallesham, P. Sudarsanam, G. Raju, B.M. Reddy, Green Chem. 15 (2013)478–489.
- [10]. S. Sandesh, G.V. Shanbhag, A.B. Halgeri, Rsc Adv. 4 (2014) 974–977.
- [11]. G. Vicente, J.A. Melero, G. Morales, M. Paniagua, E. Martin, Green Chem. 12(2010) 899–907.
- [12]. M. Balakrishna, B. Sasikumar, S. Yadaiah, A. Hari Padmasri. Iosr Journal Of Applied Chemistry (Iosr-Jac). 16 (2023) 01-10.
- [13]. M. Balakrishna, B. Sasikumar, B. Srinivas, A.V.S. Sarma, A. Hari Padmasri, Microporous Mesoporous Mater. 363 (2024) 112830.
- [14]. F. Pan, X. Lu, Q. Zhu, Z. Zhang, Y. Yan, T. Wang, S. Chen, 3(7) (2015) 4058–4066.
- [15]. W. Zhang, W. Ming, S. Hu, B. Qin, J. Ma, R. Li, Materials 11(5) (2018) 651.
- [16]. R. Shoja Razavi, M. R. Loghman-Estarki, 23(4) (2012) 1097–1106.
- [17]. I. Capel Berdiell, G.B. Braghin, T. Cordero-Lanzac, Top. Catal. 66 (2023) 1418–1426.
- [18]. H. K. Gurdeep Singh, S.Yusup. A. T. Quitain, T. Kida, M. Sasaki, K. W. Cheah And M. Ameen, Environ. Sci. Pollut. Res. 26 (2019) 34039–34046.
- [19]. S. Bordiga, C. Lamberti, F. Bonino, A. Travert, F. Thibault-Starzyk, Chemical Society Reviews, 44 (2015) 7262-7341.
- [20]. M. Król, W. Mozgawa, K. Barczyk, T. Bajda And M. Kozanecki, J. Appl. Spect., 80(5) (2013) 644-650.
- [21]. I. Pala-Rosas, J.L. Contreras, J. Salmones, R. López-Medina, D. Angeles-Beltrán, B. Zeifert, J. Navarrete-Bolaños, N.N. González-Hernández, Catalysts 13 (2023) 652.
- [22]. E. Selli, L. Forni, Microporous And Mesoporous Materials, 31 (1999) 129-140.
- [23]. P.K. Dutta, J. Twu, J. Phys. Chem. 95 (1991) 2498–2501.
- [24]. M.R. Nanda, Y. Zhang, Z. Yuan, W. Qin, H.S. Ghaziaskar, C. C. Xu, Ren.Sus. Ener. Rev. 56 (2016) 1022–1031.